Check for updates

Investigation of temperature and temporal stability of AlGaAsSb avalanche photodiodes

SALMAN ABDULLAH,[1] CHEE HING TAN,[1,*] XINXIN ZHOU,[1,2] SHIYONG ZHANG,[1,3] LUCAS PINEL,[1] AND JO SHIEN NG[1]

[1]*Department of Electrical and Electronic Engineering, University of Sheffield-North Campus, Wheeldon Street, S3 7HQ, UK*
[2]*Present address: Oclaro Technology Limited, Caswell, Towcester, NN12 8EQ, UK*
[3]*EPSRC National Epitaxy Facility, University of Sheffield-North Campus, Wheeldon Street, S3 7HQ, UK*
*c.h.tan@sheffield.ac.uk

Abstract: Since avalanche gain and breakdown voltage in most semiconductor materials change with temperature, instruments utilizing Avalanche Photodiodes (APDs) for their avalanche gains need to incorporate either temperature stabilization or voltage adjustment in the APD operation circuits. In this work we evaluated the temperature and temporal stability of avalanche gain in $Al_{0.85}Ga_{0.15}As_{0.56}Sb_{0.44}$, a wide bandgap semiconductor lattice-matched to InP substrates. We investigated the temperature and temporal stability of the gain and breakdown voltage at temperatures of 24 °C (room temperature) to 80 °C. The breakdown voltage varies linearly with temperature with a temperature coefficient of 1.60 mV/K. The avalanche gain reduces from 10 to 8.5, a reduction of 15%, when the temperature increases from 24 to 80°C. The temporal stability of gain was recorded when the APD was biased to achieve an avalanche gain of 10. Fluctuations are within ± 0.7% at 24°C, increasing to ± 1.33% at 80°C. The temperature and temporal stability of avalanche gain indicates the potential of using $Al_{0.85}Ga_{0.15}As_{0.56}Sb_{0.44}$ APDs grown on InP substrates to achieve high tolerance to temperature fluctuation.

OCIS codes: (040.1345) Avalanche photodiodes (APDs); (060.2330) Fiber optics communications.

References and links

1. S. M. Cho and H. H. Lee, "Impact ionization coefficient and energy distribution function in polar and nonpolar semiconductors," J. Appl. Phys. **71**(3), 1298–1305 (1992).
2. L. Tirino, M. Weber, K. F. Brennan, E. Bellotti, and M. Goano, "Temperature dependence of the impact ionization coefficients in GaAs, cubic SiC, and zinc-blende GaN," J. Appl. Phys. **94**(1), 423–430 (2003).
3. B. F. Levine, R. N. Sacks, J. Ko, M. Jazwiecki, J. A. Valdmanis, D. Gunther, and J. H. Meier, "A New Planar InGaAs-InAlAs Avalanche Photodiode," IEEE Photonics Technol. Lett. **18**(18), 1898–1900 (2006).
4. L. J. J. Tan, J. S. Ng, C. H. Tan, and J. P. R. David, "Avalanche Noise Characteristics in Submicron InP Diodes," IEEE J. Quantum Electron. **44**(4), 378–382 (2008).
5. L. J. J. Tan, D. S. G. Ong, J. S. Ng, C. H. Tan, S. K. Jones, Y. Qian, and J. P. R. David, "Temperature Dependence of Avalanche Breakdown in InP and InAlAs," IEEE J. Quantum Electron. **46**(8), 1153–1157 (2010).
6. X. Meng, S. Xie, X. Zhou, N. Calandri, M. Sanzaro, A. Tosi, C. H. Tan, and J. S. Ng, "InGaAs/InAlAs single photon avalanche diode for 1550 nm photons," R. Soc. Open Sci. **3**(3), 150584 (2016).
7. X. Zhou, C. H. Tan, S. Zhang, M. Moreno, S. Xie, S. Abdullah, and J. S. Ng, "Thin $Al_{1-x}Ga_xAs_{0.56}Sb_{0.44}$ Diodes with Extremely Weak Temperature Dependence of Avalanche Breakdown," R. Soc. Open Sci. **4**(5), 170071 (2017).
8. J. Xie, S. Xie, R. C. Tozer, and C. H. Tan, "Excess Noise Characteristics of Thin AlAsSb APDs," IEEE Trans. Electron Dev. **59**(5), 1475–1479 (2012).
9. X. Zhou, L. L. G. Pinel, S. J. Dimler, S. Zhang, J. S. Ng, and C. H. Tan, "Thin $Al_{1-x}Ga_xAs_{0.56}Sb_{0.44}$ Diodes With Low Excess Noise," IEEE J. Sel. Top. Quantum Electron. **24**(2), 1 (2018).
10. M. Guden and J. Piprek, "Material parameters of quaternary III - V semiconductors for multilayer mirrors at 1.55 μm wavelength," Model. Simul. Mater. Sci. Eng. **4**(4), 349–357 (1996).

11. T. Kagawa and G. Motosugi, "AlGaAsSb Avalanche Photodiodes for 1.0–1.3 μm Wavelength Region," Jpn. J. Appl. Phys. **18**(12), 2317–2318 (1979).
12. S. Miura, T. Mikawa, H. Kuwatsuka, N. Yasuoka, T. Tanahashi, and O. Wada, "AlGaSb avalanche photodiode exhibiting a very low excess noise factor," Appl. Phys. Lett. **54**(24), 2422–2423 (1989).
13. M. Grzesik, J. Donnelly, E. Duerr, M. Manfra, M. Diagne, R. Bailey, G. Turner, and W. Goodhue, "Impact ionization in $Al_xGa_{1-x}As_ySb_{1-y}$ avalanche photodiodes," Appl. Phys. Lett. **104**(16), 162103 (2014).
14. M. E. Woodson, M. Ren, S. J. Maddox, Y. Chen, S. R. Bank, and J. C. Campbell, "Low-noise AlInAsSb avalanche photodiode," Appl. Phys. Lett. **108**(8), 081102 (2016).
15. L. L. G. Pinel, *et al.*, "Improving Wet Etching of InGaAs/AlGaAsSb Avalanche Photodiode," in *19th International Conference on Molecular Beam Epitaxy* (2016).
16. M. H. Woods, W. C. Johnson, and M. A. Lampert, "Use of a Schottky barrier to measure impact ionization coefficients in semiconductors," Solid-State Electron. **16**(3), 381–394 (1973).
17. Hamamatsu Photonics Data sheets for S6045 and S5344, Si APDs. Hamamatsu Photonics Inc., March 2014.
18. F. Ma, G. Karve, X. Zheng, X. Sun, A. L. Holmes, Jr., and J. C. Campbell, "Low-temperature breakdown properties of $Al_xGa_{1-x}As$ avalanche photodiodes," Appl. Phys. Lett. **81**(10), 1908–1910 (2002).
19. J. S. L. Ong, J. S. Ng, A. B. Krysa, and J. P. R. David, "Temperature dependence of avalanche multiplication and breakdown voltage in $Al_{0.52}In_{0.48}P$," J. Appl. Phys. **115**(6), 064507 (2014).
20. D. J. Massey, J. P. R. David, and G. J. Rees, "Temperature dependence of impact ionization in submicrometer silicon devices," IEEE Trans. Electron Dev. **53**(9), 2328–2334 (2006).
21. S. Xie and C. H. Tan, "AlAsSb Avalanche Photodiodes With a Sub-mV/K Temperature Coefficient of Breakdown Voltage," IEEE J. Quantum Electron. **47**(11), 1391–1395 (2011).
22. D. S. G. Ong, J. S. Ng, Y. L. Goh, C. H. Tan, S. Zhang, and J. P. R. David, "InAlAs Avalanche Photodiode With Type-II Superlattice Absorber for Detection Beyond 2 μm," IEEE Trans. Electron Dev. **58**(2), 486–489 (2011).

1. Introduction

Avalanche Photodiodes (APDs) are routinely used in optical detection systems, transforming weak optical signals into large photocurrents such that the signals are significantly larger than noise originating from electronics. The signal amplification is achieved by a mechanism called impact ionization. When a photo-generated electron (or hole) injected into a high electric field region accumulates sufficient energy from the electric field, it may trigger an impact ionization collision with atoms of the semiconductor material, producing a new electron-hole pairs. A series of such impact ionization events results in amplification of the signal, which is usually termed as avalanche gain or multiplication factor, *M*.

Ideally the electrons (or holes) gain energy from the electric field without encountering energy loss scattering collisions with phonons, so that subsequent impact ionization events occur soon after the original event. In reality, however, there exist a number of scattering mechanisms, which reduce and randomize the electron's energy. In semiconductors such as GaAs, the inter- and intra-valley phonon scatterings are dominant at high electric fields [1]. These phonon populations increase strongly with temperature, *T*, acting to regulate the population of hot electrons and holes with high likelihood to initiate impact ionization events. Consequently, the rate of impact ionization, the avalanche gain and the breakdown voltage, V_{bd}, are usually strongly dependent on temperature [2].

In practical terms, the temperature stability of APDs are often characterized by the temperature coefficients of *M* and V_{bd}, defined as dM/dT and $C_{bd} = dV_{bd}/dT$, respectively. In addition to temperature stability, good temporal stability is required to yield a constant output signal for practical use in long haul telecom networks. In long haul optical networks, the low loss window at 1550 nm wavelength has been the driving force behind the use of InGaAs-based photodiodes and APDs. Current commercial APDs employ InGaAs absorption layer and an InP avalanche layer. In the past decade, InAlAs, which has a wider bandgap than InP, has attracted interest as an alternative avalanche material, because of its much smaller C_{bd} than those of InP [3], amongst its other advantages such as lower band-to-band tunnelling current than InP [4] and lower excess noise factor [5]. For example, a 100 nm thick InAlAs APD gives C_{bd} of 2.5 mV/K compared to the 6 mV/K from an 130 nm thick InP APD [5]. InAlAs has also been employed in 1550 nm wavelength single photon avalanche diodes, whose V_{bd} varies by < 0.2 V over a 30 K change in temperature [6].

The benefits of using wider bandgap materials as avalanche layer have also been observed in $Al_{1-x}Ga_xAs_{0.56}Sb_{0.44}$ (x = 0 to 0.15) grown lattice matched to InP substrates. Based on data obtained at 77 to 297 K, $Al_{1-x}Ga_xAs_{0.56}Sb_{0.44}$ APDs with ~100 nm thick avalanche layers exhibit small C_{bd} values of 0.86-1.08 mV/K, without signs of significant band-to-band tunnelling current [7]. These APDs also produce very low excess noise characteristics, with effective ionization coefficient ratios k_{eff} of 0.05-0.1 [8,9]. The $Al_{1-x}Ga_xAs_{0.56}Sb_{0.44}$ APDs reported in [8–10] are superior to and distinct from earlier $Al_{1-x}Ga_xAs_{1-y}Sb_y$ APDs (x > 0.7 and y > 0.89), which are lattice-matched to GaSb substrates. The latter have narrower bandgaps (0.7-1.2 eV) [10] and much thicker avalanche layers (several microns) [11], which gave higher excess noise k_{eff} of 0.2 [12] and C_{bd} ~30 mV/K in a 700 nm avalanche region [13]. Recently $Al_{0.7}In_{0.3}As_{0.3}Sb_{0.7}$ APDs grown on GaSb substrate have also been reported with promising low noise [14].

In this work, we report our experimental study on the $Al_{0.85}Ga_{0.15}As_{0.56}Sb_{0.44}$ APDs (lattice-matched to InP substrates), focusing on the stability of avalanche gain at above room temperature, not previously covered by the temperature range used in ref [7]. Our study also covers temporal stability of avalanche gain, with comparison to commercial Si APDs.

2. Device fabrication and experimental details

The $Al_{0.85}Ga_{0.15}As_{0.56}Sb_{0.44}$ APD sample used in this work was fabricated from a wafer grown by molecular beam epitaxy on an n^+ InP substrate. The wafer structure, shown schematically in Fig. 1(a), consists of a nominally 100 nm thick unintentionally doped $Al_{0.85}Ga_{0.15}As_{0.56}Sb_{0.44}$ layer, which is sandwiched between a 100 nm thick Te-doped n-type $Al_{0.85}Ga_{0.15}As_{0.56}Sb_{0.44}$ layer and a 300 nm Be-doped p-type $Al_{0.85}Ga_{0.15}As_{0.56}Sb_{0.44}$ layer. Highly doped n- and p-$In_{0.47}Ga_{0.53}As$ layers are included to facilitate good ohmic contacts for fabricated devices. Device fabrication using conventional UV-photolithography and wet chemical etching produced circular mesa diodes with optical windows, as shown in Fig. 1(b). A citric acid solution and a diluted hydrochloric acid solution were used to etch the $In_{0.47}Ga_{0.53}As$ layers and the $Al_{0.85}Ga_{0.15}As_{0.56}Sb_{0.44}$ layers, respectively [15]. Ti/Au (20 nm/200 nm) contacts were deposited to form p and n ohmic contacts for the devices. Finally a negative photoresist SU-8 was deposited to protect the mesa sidewalls. There was no antireflection coating in the fabricated devices.

Most of the measurements were performed on APDs with diameters of 220 µm. Characterization of the devices began with dark current-voltage (*I-V)* measurements. APDs with low surface dark current and well-defined breakdown voltage were selected for subsequent avalanche gain, high temperature and temporal stability measurements. To measure avalanche gain, the device-under-test (DUT) was illuminated by a continuous-wave 633 nm wavelength He-Ne laser to generate photocurrent. Emission from the laser was mechanically chopped at 180 Hz, before being focused onto the optical window of the DUT. Using a commercial Si photodiode (BPX-65), it was verified that the laser power (46 µW) remained stable within ± 0.5% over typical duration of our measurements. A lock-in amplifier (model SR830) was used for phase-sensitive detection of the photocurrent, minimizing effects from device's dark current and background radiation. Care was taken to focus the light to the centre of the mesa diode to avoid absorption of light at the mesa sidewall. Measurements on diodes with diameters of 220 and 120 µm produced similar photocurrent and avalanche gain, confirming that the focused laser spot was smaller than 120 µm. Since the laser was confined to the center of the mesa diode, the measured avalanche gain was not affected by possible premature sidewall breakdown. Values of M versus reverse bias are given by the ratio of photocurrent data to the injected photocurrent. The latter as function of reverse bias was estimated by extrapolating values of photocurrent at low reverse bias (where no avalanche gain occurs) to higher reverse bias [16].

For elevated temperature measurements, the APD was placed on a heated copper plate. The temperature was monitored using a thermocouple sensor and the current supply to the

copper plate was controlled to achieve the desired temperature. Multiple sets of measurement taken indicated that temperature gradient between the copper plate and DUT was insignificant. A LabVIEW program was used to collect the photocurrent in DUT as a function of time for the temporal stability characterization at room and higher temperatures. The data collected included fluctuations due to laser or other equipment (if present).
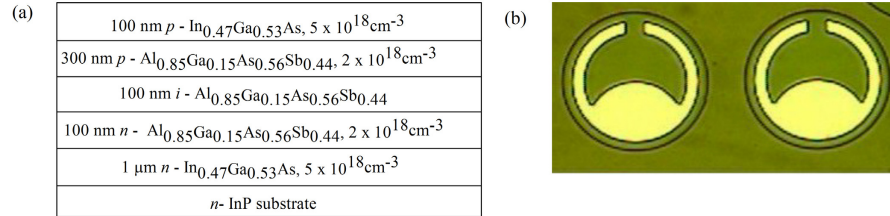
(a)

| 100 nm p - In$_{0.47}$Ga$_{0.53}$As, 5 x 10^{18}cm^{-3} |
| 300 nm p - Al$_{0.85}$Ga$_{0.15}$As$_{0.56}$Sb$_{0.44}$, 2 x 10^{18}cm^{-3} |
| 100 nm i - Al$_{0.85}$Ga$_{0.15}$As$_{0.56}$Sb$_{0.44}$ |
| 100 nm n - Al$_{0.85}$Ga$_{0.15}$As$_{0.56}$Sb$_{0.44}$, 2 x 10^{18}cm^{-3} |
| 1 µm n - In$_{0.47}$Ga$_{0.53}$As, 5 x 10^{18}cm^{-3} |
| n- InP substrate |

(b)

Fig. 1. (a) Wafer structure and (b) top view of circular mesa diodes with 220 µm diameter used in this work.

3. Results and discussion

Dark currents from 27 APDs with diameter of 220 µm are shown in Fig. 2 (a). The spread in the dark current prior to breakdown indicates presence of surface leakage current. However all diodes breakdown at similar voltage values. Avalanche gain characteristics of four selected devices, namely APD-1, 2, 3 and 4, are plotted in Fig. 2 (b). At 11.9 V, the corresponding M values are 10.46, 10.28, 10.38, and 9.90. The gain data for the four selected APDs at different temperatures are plotted as $1/M$ versus reverse bias in Fig. 3, so that V_{bd} can be extracted by extrapolating $1/M$ to zero. The mean breakdown voltage at room temperature (24 °C) is 12.41. At 24, 40, 60 and 80 °C, the mean breakdown voltages obtained are 12.41, 12.43, 12.47 and 12.50 V, respectively. As temperature increases, M decreases hence the breakdown voltage increases slightly. We observed that V_{bd} varies linearly with temperature within our measurement range and can be fitted by $V_{bd} = C_{bd}T + 12.36$, where $C_{bd} = 1.60$ mV/K.
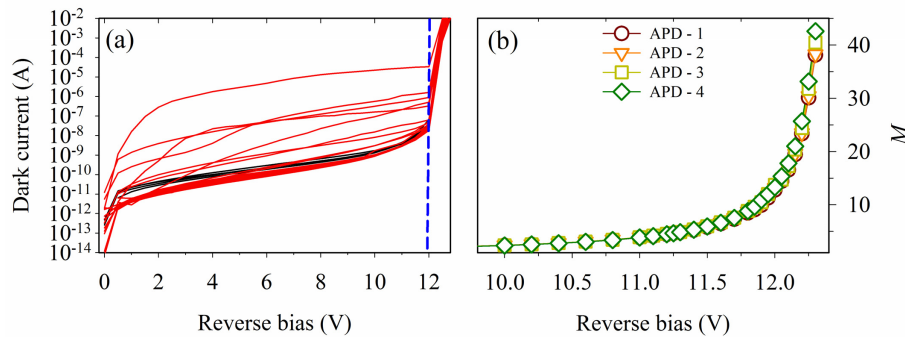

Fig. 2. (a) Room temperature dark currents of 27 APDs with diameter of 220 µm. Data of four APDs selected for subsequent high temperature measurement are plotted in black solid lines. Blue reference line indicates −11.9 V reverse bias. (b) Measured gain at room temperature from the four selected APDs.

Small C_{bd} values have also been reported for Al$_{0.6}$Ga$_{0.4}$As [18] and Al$_{0.52}$In$_{0.48}$P [19]. Dominance of alloy scattering has been proposed as the reason for small C_{bd} in these materials. Analyzing the AlAs$_{0.56}$Sb$_{0.44}$ alloy, ref [20]. found large difference in covalent radii of As and Sb, indicating a strong alloy disorder potential and hence a dominant alloy scattering that is temperature insensitive. Since the ratio of covalent radii between As and Sb atoms is identical for Al$_{1-x}$Ga$_x$As$_{0.56}$Sb$_{0.44}$ and AlAs$_{0.56}$Sb$_{0.44}$, we can also expect a small C_{bd} for the Al$_{1-x}$Ga$_x$As$_{0.56}$Sb$_{0.44}$ alloys. In addition, C_{bd} is small for thin APDs [20], which operate

at very high electric fields where carriers experience reduced phonon scattering events. Therefore, the $Al_{0.85}Ga_{0.15}As_{0.56}Sb_{0.44}$ APD of this work combines dominant alloy scattering in the material and reduced phonon scattering at high electric field (~1000 kV/cm). These are two likely contributing factors for the small C_{bd} values [21].
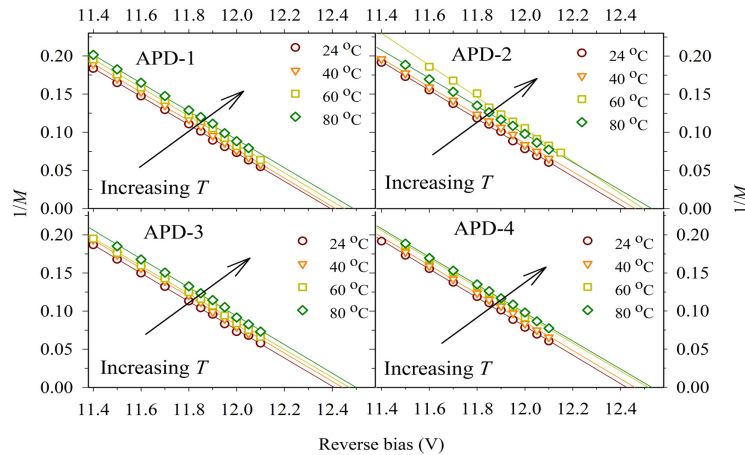

Fig. 3. 1/M plotted as a function of reverse bias for each APD. Solid lines represent linear fit to the experimental data.

Data of temporal stability of gain from the four selected APDs are shown in Fig. 4. All were measured at 11.9 V reverse bias and each set was collected over 12.5 minutes. The data are presented as percentage fluctuations with reference to mean gain obtained at 11.9 V. AT room temperature, the fluctuation of M is ± 0.5%. As temperature increases, the fluctuations of M are within ± 1.1% for all devices over the range of temperatures studied, except for APD-1, which shows a maximum fluctuation of + 1.33% at 80 °C. No particular trend in temporal drift in M was observed.
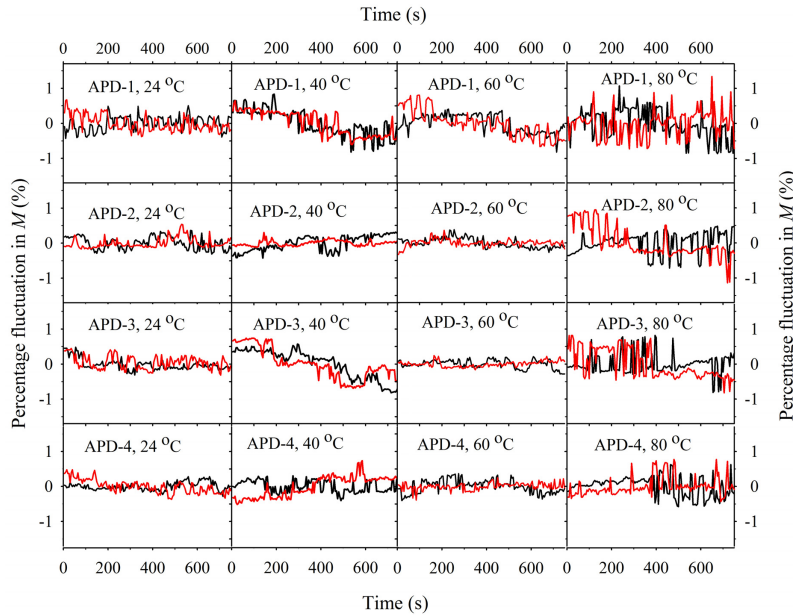
Fig. 4. Fluctuations of M versus time for APD-1, -2, -3 and -4, at 24, 40, 60 and 80 °C, with reference to mean gain values at respective temperatures at 11.9 V. Two sets of data were recorded for each APD at a given temperature.
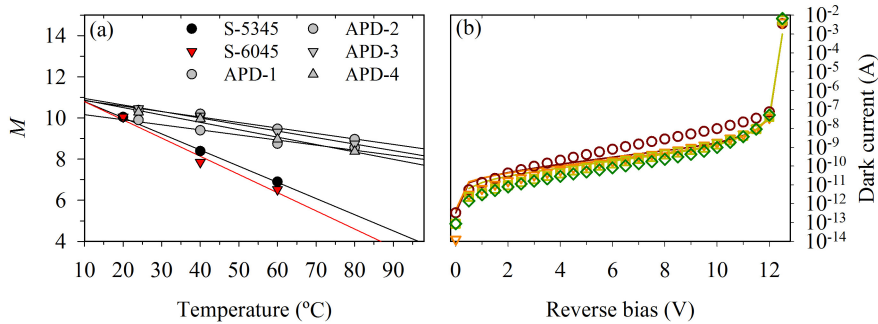

Fig. 5. (a) Comparison of M versus temperature between the $Al_{0.85}Ga_{0.15}As_{0.56}Sb_{0.44}$ APDs and commercial Si APDs. Solid lines are linear fittings to the data. (b) Dark currents of the four $Al_{0.85}Ga_{0.15}As_{0.56}Sb_{0.44}$ APDs before (lines) and after (symbols) temperature dependence measurements.

Using the gain data at 11.9 V from the four $Al_{0.85}Ga_{0.15}As_{0.56}Sb_{0.44}$ APDs, a comparison is then made with performance of the two commercial Si APDs, as shown in Fig. 5 (a). The data for the Si APDs were extracted from their data sheets [17]. As temperature increases, gain reduces in all six APDs, with much smaller reduction in the four $Al_{0.85}Ga_{0.15}As_{0.56}Sb_{0.44}$ APDs than in the Si APDs. Based on linear fittings to the data, from 24 to 80 °C, M reduces by 15, 45, and 52% for the $Al_{0.85}Ga_{0.15}As_{0.56}Sb_{0.44}$ APDs, the S5345 Si APD, and the S6045 Si APD, respectively.

With only a small reduction in gain, there is potential in simplifying the APD biasing circuit design, if using the $Al_{0.85}Ga_{0.15}As_{0.56}Sb_{0.44}$ APDs. Since $Al_{0.85}Ga_{0.15}As_{0.56}Sb_{0.44}$ is lattice-matched to InP substrates, it has the potential to replace InP or InAlAs as the avalanche material for APDs operating at infrared wavelengths up to 1600 (using InGaAs absorber) or 2300 nm (using InGaAs/GaAsSb Type II superlattice absorber [22]). We also recorded the dark currents of the $Al_{0.85}Ga_{0.15}As_{0.56}Sb_{0.44}$ APDs before and after the gain

measurements at elevated temperatures, which are compared in Fig. 5 (b). No significant degradation in the dark currents was observed.

4. Conclusion

Temperature and temporal stability of avalanche gain in $Al_{0.85}Ga_{0.15}As_{0.56}Sb_{0.44}$ APDs were studied experimentally at 24 to 80 °C. The temperature coefficient of breakdown voltage was found to be a very low 1.60 mV/K. When operated to give a mean gain of 10, the APDs produced avalanche gains with a maximum fluctuation of ± 0.5% over 12.5 minutes at 24 °C. Measurements were repeated at 40, 60 and 80 °C. At the highest temperature of 80 °C, the maximum fluctuation of 1.33% was recorded. As temperature increases the gain drops. When compared to data from commercial Si APDs, our APDs with thin $Al_{0.85}Ga_{0.15}As_{0.56}Sb_{0.44}$ avalanche layer show smaller sensitivity to temperature. No significant degradation was observed in dark current. These results suggest that a thin $Al_{0.85}Ga_{0.15}As_{0.56}Sb_{0.44}$ avalanche layer could be employed in APDs for temperature tolerance.